ALMA MATER STUDIORUM
UNIVERSITÀ DI BOLOGNA

ARCHIVIO ISTITUZIONALE
DELLA RICERCA

Alma Mater Studiorum Università di Bologna
Archivio istituzionale della ricerca

The double exciton state of conjugated chromophores with strong diradical character: insights from TDDFT calculations

This is the final peer-reviewed author's accepted manuscript (postprint) of the following publication:

Published Version:
Canola, S., Casado, J., Negri, F. (2018). The double exciton state of conjugated chromophores with strong diradical character: insights from TDDFT calculations. PHYSICAL CHEMISTRY CHEMICAL PHYSICS, 20(37), 24227-24238 [10.1039/C8CP04008G].

Availability:
This version is available at: https://hdl.handle.net/11585/657403 since: 2020-02-25

Published:
DOI: http://doi.org/10.1039/C8CP04008G

Terms of use:

Some rights reserved. The terms and conditions for the reuse of this version of the manuscript are specified in the publishing policy. For all terms of use and more information see the publisher's website.

This item was downloaded from IRIS Università di Bologna (https://cris.unibo.it/).
When citing, please refer to the published version.

(Article begins on next page)

12 October 2024

This is the final peer-reviewed accepted manuscript of:

S. Canola, J. Casado, F. Negri," The double exciton state of conjugated chromophores with strong diradical character: insights from TDDFT calculations", Phys. Chem. Chem. Phys., **20** (2018), 24227-24238. The final published version is available online at: DOI: 10.1039/c8cp04008g

Rights / License:

The terms and conditions for the reuse of this version of the manuscript are specified in the publishing policy. For all terms of use and more information see the publisher's website.

This item was downloaded from IRIS Università di Bologna (https://cris.unibo.it/)

When citing, please refer to the published version.

The double exciton state of conjugated chromophores with strong diradical character: insights from TDDFT calculations

Sofia Canola,[a,b] Juan Casado[c] and Fabrizia Negri[a,b]

A peculiar characteristic of open-shell singlet diradical molecules is the presence of a double exciton state (H,H→L,L) among low lying excited states. Recent high-level quantum-chemical investigations including static and dynamic electron correlation have demonstrated that this state can become the lowest singlet excited state, a diagnostic fingerprint of the diradical system. Here we investigate the performance of less computationally demanding TDDFT calculations by employing two approaches: the spin-flip TDDFT scheme and TD calculations based on unrestricted broken symmetry antiparallel-spin reference configuration (TDUDFT). The calculations are tested on a number of recently synthesized, large conjugated systems displaying from moderate to large diradical character and showing experimental trace of the double exciton state. We show that spin-flip (SF) TDB3LYP calculations in the collinear approximation generally underestimate the excitation energy of the double exciton state. When the molecule displays a strong diradical character, the unrestricted antiparallel-spin reference configuration of TDUDFT calculations is characterized by strongly localized frontier molecular orbitals. We show that under these conditions the double exciton state is captured by TDUB3LYP calculations since it is described by singly excited configurations and its excitation energy can be accurately predicted. Owing to the improved description of the ground state, also the excitation energy of the single exciton H→L state generally improves at TDUB3LYP level. As regard the double exciton state, SF TDB3LYP performs slightly better for small to medium diradical character while a large diradical character, (and strong orbital localization) is a prerequisite for the success of TDUB3LYP calculations whose quality otherwise deteriorates.

Introduction

Open-shell singlet diradicals have attracted remarkable interest in recent years, due to their unique electronic properties which include narrow singlet-triplet gap, moderate to high charge carrier mobilities and ambipolar charge transport behavior, along with optical and magnetic properties suitable for applications in nonlinear optics, molecular spintronics and energy storage devices.[1-5]

A distinctive electronic character of these systems is a small HOMO-LUMO (H-L) gap which is in turn associated with their ambipolar conduction properties,[6] their electronic absorption toward the NIR and also with their possible application in singlet fission [7-10].

These unique properties are modulated by their diradical character, a quantum-chemical index which was originally defined as twice the weight of the double excitation configuration in the multiconfiguration self-consistent- field (MC-SCF) method [11]. It can be computed from spin-unrestricted approaches [12] but it has also been connected to experimental observables. [13]

A large number of conjugated chromophores with open shell singlet ground state have been designed an synthesised recently,[14,15] displaying from moderate to large diradical character, encompassing quinoidal oligo thiophenes [16-18], tetracyano quinodimethane derivatives of phenylene-vinylenes [19], diphenalenyl compounds [13,20] several polycyclic aromatic hydrocarbons [14,21-26], heteroacenes [27,28], among others. For most of these systems the diradical character can be rationalized by considering the recovery of aromaticity (i.e., the gaining of Clar´s sextets) [2].

Owing to the small H-L gap, the electronic structure of open shell singlet diradicals is significantly influenced by the role of static correlation and multi-reference models are generally required. Alternatives to MCSCF have been proposed such as the restricted active space spin-flip (RAS-SF) approach, employed to predict the multi-reference nature of organic polyradicals[29], the singlet-triplet energy difference in carbazole macrocycles with polyradical characters [30] and the radical character in linear and cyclic oligoacenes [31]. The multireference averaged quadratic coupled cluster (MRAQCC) method has also been employed to predict the multiradical character of model systems for graphene nanoflakes [32] and zethrenes. [33]

To describe the singlet ground state of open-shell diradicals also spin-unrestricted Hartree–Fock (UHF) and density functional theory (UDFT) methods have been largely employed.[34] Indeed, the restricted closed shell (CS) approach generally leads to an instability and a lower energy open-shell antiparallel-spin solution, characterized by broken symmetry (BS) of the electronic wavefunction, is found at unrestricted level of theory.

The simplest quantum-chemical model to describe a diradical includes two electrons in two orbitals (2e-2o) from which four electronic states can be constructed: three singlets and one

[a.] *Università di Bologna, Dipartimento di Chimica 'G. Ciamician', Via F. Selmi, 2, 40126 Bologna, Italy.*
[b.] *INSTM, UdR Bologna, Italy. E-mail: fabrizia.negri@unibo.it*
[c.] *Department of Physical Chemistry, University of Málaga, Andalucia-Tech, Campus de Teatinos s/n, 29071 Málaga, Spain.*

Electronic Supplementary Information (ESI) available: [figures with equilibrium structures, molecular orbitals from restricted and unrestricted approaches, tables including absolute energies, tetraradical character, excitation energies and other details on computed excited states]. See DOI: 10.1039/x0xx00000x

triplet. The spatial wavefunctions of the four electronic states were derived either by assuming a set of delocalized orbitals or a set of localized orbitals [8,35-37]. In the delocalized orbital basis, the lowest singlet state is described by the ground configuration corrected with the doubly excited (H,H→L,L) configuration [36,37]. The second singlet state is a singly excited or single exciton (H→L) state and the third is dominated by the doubly excited (H,H→L,L) configuration and is therefore a double exciton state.

According to the 2e-2o model, the double exciton state is found at higher energy than the single exciton state. [8, 36] However, some of us have shown recently, via CASPT2//CASSCF calculations [38] that for some systems displaying remarkable diradical character, the double exciton state becomes the lowest energy excited singlet state, a peculiarity which is well known for the class of polyenes.[39] Similarly to the latter, the double exciton state of open-shell singlet diradicals is generally one-photon forbidden or only weakly allowed and it appears in the optical spectra as a weak band or progression on the red side of the main strong absorption band which is due to the strongly allowed single exciton state.[38, 40]

In previous studies, CASSCF followed by CASPT2 calculations were chosen to account for static and dynamic electron correlation and allowed to find a close agreement with the experimental excitation energy of the double exciton state of quinoidal oligothiophenes [38] and, more recently, of tetracyano quinodimethane derivatives of phenylene-vinylenes [40]. Similarly, CASSCF followed by NEVPT2 calculations were recently carried out for quarteranthene [21]. These calculations however, can become rapidly unfeasible with the required accuracy, for very large molecules such as some recently synthesized open-shell singlet diradicals.

The computationally less demanding time-dependent DFT (TDDFT) calculations predict, generally with good accuracy, the excitation energies of low lying excited states [41,42] but they are limited to the inclusion of single excitations.

Spin flip (SF) TDDFT[43,44] offers the advantage that, among the single excitations generated starting from the triplet reference configuration, the double excitation (with respect to the singlet ground state configuration) is also included. Indeed this approach has been successfully employed to predict the excitation energy of the double exciton state of polyenes[45].

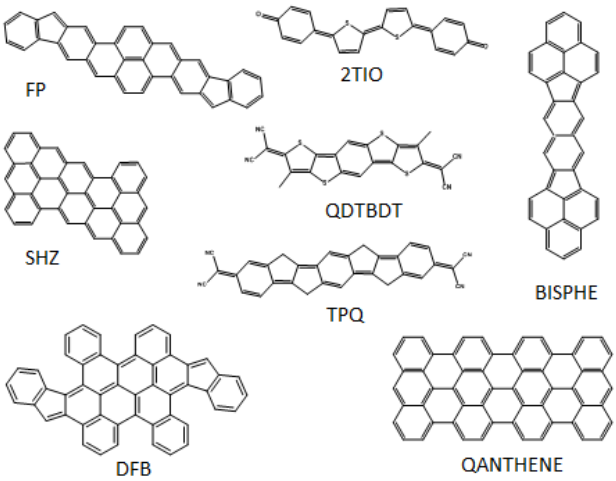

Fig. 1. Structural formula of the molecular systems investigated in this work, displaying from medium to very large diradical character.

Concerning standard TDDFT calculations, the use of a BS spin unrestricted reference configuration with antiparallel spins is also a possible choice. Interestingly the BS solution is characterized by alpha and beta frontier molecular orbitals (MOs) localized on two different spatial regions of the molecule, in analogy with the localized basis set employed as an alternative to the delocalized basis set, in the formulation of the 2e-2o model [36]. Here we show that the wavefunction of the double exciton state is described in terms of singly excited configurations, when the reference open-shell BS configuration is formed by strongly localized frontier MOs. Therefore we propose that, as far as the simple 2e-2o approach holds, and the BS frontier MOs are well localized, a viable alternative to study the low lying electronic excited states of large conjugated diradicals and, more precisely, to identify and locate the double exciton state which characterizes them, is to perform TDDFT calculations based on the unrestricted BS antiparallel-spin reference configuration, a procedure hereafter labelled TDUDFT. We note that also SF TDDFT calculations are based on an unrestricted (parallel-spin or triplet) reference configuration but in the following we choose to label TDUDFT only the approach using as a reference an unrestricted antiparallel-spin configuration. To explore the validity of this approach, we considered a number of open-shell singlet diradicals recently synthesized [13,18,19, 21,23,24,26,27] and whose models are shown in Fig. 1. For six out of the eight molecules, the electronic spectra show weak features on the red side of the main strong absorption band which have been assigned to the double exciton state either based on high level calculations [21,38,40] or for analogy. In one case [27] the spectrum shows weak features in the red side of the main absorption band that have not been assigned and in another case [13] a dark state has been identified but at slightly higher energies than the bright state. For these systems we determined the equilibrium structures employing both CS DFT and BS UDFT approaches, evaluated their diradical and multiradical character and carried out a systematic investigation of excitation energies at TDDFT and TDUDFT

level, paying particular attention to the prediction of the double exciton state when the open-shell BS antiparallel-spin reference configuration is employed. We complemented these investigations with SF TDDFT calculations and compared the results of the two approaches with available experimental data.

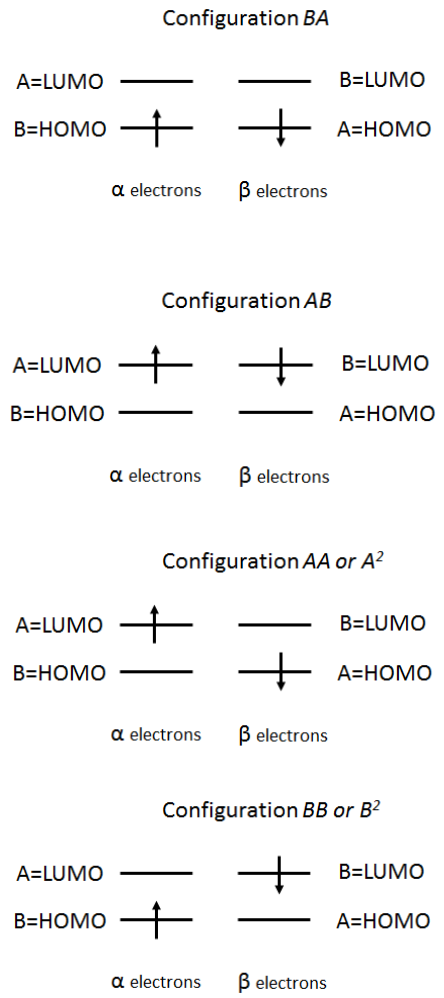

Fig. 2. Correspondence between the notation *A,B* of localized orbitals in the 2e-2o model and the localized HOMOα,β and LUMOα,β orbitals from UDFT calculations on diradical systems with large diradical character.

Modelling the electronic structure of open-shell singlet diradicals

In the following calculations two main simplifying assumptions were made. The molecules shown in Fig. 1 did not include the substituents of the real molecules since these contribute only marginally to the final structural and electronic properties of the extended conjugated chromophores. Although solvent effects may improve the accuracy of predictions, they were not considered because most experimental data, used for comparison with calculations, were obtained with the same solvent and because excitation energies were computed for models and not for the real molecules. Both simplifications can introduce systematic errors in the estimated energies but the focus of this work is rather on the suitability of TDDFT approaches to describe the double exciton state and their suitability as a function of the diradical character. With regard to the structural simplifications assumed for the model molecules, 2TIO did not include the tert-butyl substituents; QDTBDT included methyl substituents instead of the branched alkyl chains; FP did not include the mesityl and O-alkyl substituents; DFB did not include tert-butyl and mesityl substituents; BISPHE did not include tert-butyl and phenyl substituents; TPQ did not include aryl and phenyl substituents; SHZ did not include aryl, methyl and tert-butyl substituents; QANTHENE did not include tert-butyl and aryl substituents.

The open-shell singlet ground state

The equilibrium structures of the molecules shown in Fig. 1 were determined with DFT calculations employing the B3LYP and CAM-B3LYP functionals and the 6-31G* basis set. The geometry optimization was first carried out with the restricted approach to determine a CS equilibrium structure. For all the systems investigated a more stable open-shell BS solution was found at the CS geometry and therefore the equilibrium structure corresponding to the BS solution was readily determined. In the following we will refer to this structure as the BS equilibrium structure although it should be clear that the BS is referred to the electronic wavefunction and not to the atomic structure. The overall CS-BS stability was determined as the energy difference between the energy of the CS structure computed with restricted DFT and the energy of the BS structure computed with UDFT. At both CS and BS geometries the diradical and tetraradical character was determined in the spin-unrestricted single determinant formalism with the spin-projection scheme.[8,12] The diradical y_0 and tetraradical character y_1 in the PUHF formalism is obtained according to the following relation

$$y_i^{PUHF} = 1 - \frac{2T_i}{1+T_i^2} \qquad (1)$$

where

$$T_i = \frac{n_{HONO-i} - n_{LUNO+i}}{2} \qquad (2)$$

where $n_{HONO-i,LUNO+i}$ are the occupation numbers of the occupied and unoccupied natural orbitals (NO) determined at UHF level. The diradical character corresponds to $i = 0$ while the tetraradical character is obtained for $i = 1$. NO occupation numbers were also determined at UDFT level, employing the same functional used for the geometry optimization. In addition, the number of unpaired electrons N_u was determined following the formulation of Head-Gordon[46]

$$N_u = \sum_i \left(1 - abs(1 - n_i)\right) \qquad (3)$$

The lowest singlet excited states

The 2e-2o model is a useful starting point for the description of the electronic structure of diradical molecules although it is

generally an approximation. Diradicals of real interest normally contain more than two electrons and more than just two MOs are available for them. As such, the energetic order of closely spaced states described from this model can be incorrect owing to the lack of electron correlation. This model has been described in detail in fundamental contributions [35, 36] and used to rationalize non-linear optical properties of diradicals along with their suitability for singlet fission.[8]

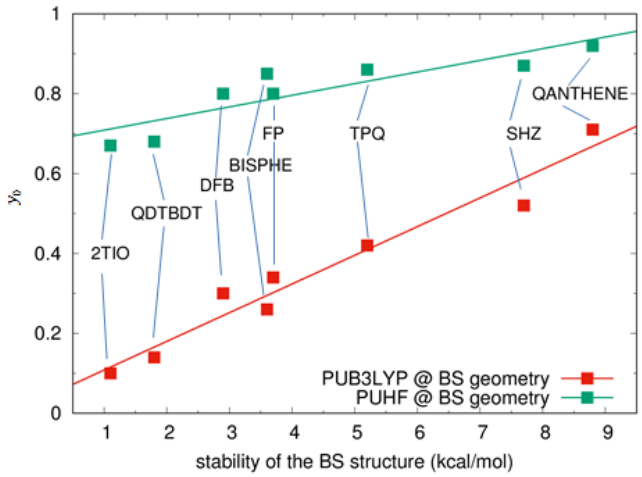

Fig. 3. Correlation between the y_0 value computed at PUHF (green squares) or PUB3LYP (red squares) level and the computed stabilization of the BS structure with respect to the CS structure, both optimized at B3LYP/6-31G* level.

Table 1 Energy difference between the BS optimized geometries and the CS optimized geometries.

	ΔE(BS-CS) kcal/mol	*ΔE(BS-CS) kcal/mol*
	*B3LYP/6-31G**	*CAM-B3LYP/6-31G**
2TIO	1.1	7.3
QDTBDT	1.8	10.5
FP	3.7	11.5
DFB	2.9	9.0
BISPHE	3.6	15.7
TPQ	5.2	17.3
SHZ	7.7	20.1
QANTHENE	8.8	21.5

Within the 2e-2o model a full CI is carried out, and therefore the results are independent of the orbital basis sets. Two limiting cases were considered[36]: a delocalized basis set a, b and a localized basis set A, B. Using the same notation as in ref.[36] we can write, for the two sets of orbitals, the following configurations with paired spins: $a(1)a(2) = a^2$; $b(1)b(2) = b^2$; $a(1)b(2) = ab$; $b(1)a(2) = ba$ in the delocalized basis and $A(1)A(2) = A^2$; $B(1)B(2) = B^2$; $A(1)B(2) = AB$; $B(1)A(2) = BA$, in the localized basis.

Table 2 Diradical character y_0 computed at different levels of theory for CS and BS optimized structures of the systems investigated. The basis set is 6-31G*

	y_0 PUHF			
geometry→	CS CAM-B3LYP	CS B3LYP	BS UCAM-B3LYP	BS UB3LYP
2TIO	0.46	0.56	0.74	0.67
QDTBDT	0.53	0.60	0.73	0.68
FP	0.62	0.71	0.81	0.80
DFB	0.65	0.73	0.81	0.80
BISPHE	0.83	0.84	0.86	0.85
TPQ	0.66	0.77	0.88	0.86
SHZ	0.78	0.83	0.87	0.87
QANTHENE	0.85	0.89	0.92	0.92
	y_0 PUCAM-B3LYP	*y_0 PUB3LYP*	*y_0 PUCAM-B3LYP*	*y_0 PUB3LYP*
geometry→	CS CAM-B3LYP	CS B3LYP	BS UCAM-B3LYP	BS UB3LYP
2TIO	0.08	0.02	0.51	0.10
QDTBDT	0.20	0.06	0.53	0.14
FP	0.19	0.13	0.63	0.34
DFB	0.21	0.12	0.54	0.30
BISPHE	0.49	0.20	0.61	0.26
TPQ	0.32	0.21	0.77	0.42
SHZ	0.51	0.40	0.71	0.52
QANTHENE	0.63	0.57	0.84	0.71

These configurations result in one triplet state and three singlet states whose spatial wavefunctions for perfect homosymmetric diradicals and assuming E(b) < E(a), are expressed as:[36]

$$S_0 = \psi_0 = b^2 - a^2 = AB + BA$$
$$S_1 = \psi_1 = ab + ba = A^2 - B^2 \qquad (4)$$
$$S_2 = \psi_2 = a^2 + b^2 = A^2 + B^2$$

Note that the S_2 state is the double exciton state in which the (H,H→L,L) excitation or a^2 in the delocalized basis, strongly contributes to the wavefunction. Within the 2e-2o model this state is predicted to be always above S_1, the (H→L) or $ab + ba$ state in the delocalized basis.

As discussed above, the ground state of open shell singlet diradical systems, displaying medium to large diradical character, whose nature is intrinsically multiconfigurational, can be described in a one determinant approach by the spin-unrestricted BS solution, usually employing DFT. Owing to the relaxed constraint, the molecular orbitals of the BS solution are localized on opposite moieties of the molecule, in contrast with the delocalized orbitals determined for the CS solution. In the light of the 2e-2o model described above, we note that CS and BS solutions obtained from standard DFT calculations correspond, to a good approximation, to the two limiting cases of a set of delocalized (the CS solution) or localized (the BS solution) MOs. When the BS orbitals are strongly localized and disjoint (which is associated with a large diradical character), the HOMO orbital holding the α electron is almost identical to the LUMO orbital computed for the β electrons and vice versa. Indeed, each spin-orbital holds just one electron of a given spin and for a pair of strongly localized HOMOα and HOMOβ orbitals there must be another pair identical to them but

holding the complementary spin. In this case there is a clear correspondence between the computed UDFT frontier MOs for α and β electrons and the localized *A,B* pair of the 2e-2o model. The four configurations of the model can be identified with the four configurations based on UDFT frontier MOs, as shown in Fig. 2.

Under these circumstances, namely strong diradical character and strongly localized BS orbitals, we can interpret the eigenstates of a TDUDFT calculation using, as a guide, the singlet excited state wavefunctions of eq.(4) from the 2e-2o model.

Comparing the open-shell singlet ground state wavefunction of eq.(4) with the results of UDFT calculations, we note, as well known, that the singlet ground state S_0 is described with the configuration BA which is not a spin eigenfunction and therefore may result in large spin-contamination. The configuration AB corresponds indeed to a double excited configuration (see Fig. 2) and it will not be recovered in TDUDFT calculations. Moving to singlet excited states, we note that both S_1 and S_2 in eq.(4) are described by ionic configurations A^2 and B^2 that correspond to single excitations from the reference BA configuration (see Fig. 2). Therefore we can conclude that, for systems with well localized frontier MOs, TDUDFT calculations can be used to predict the excitation energy of the double exciton state, besides that of the single exciton state, since both are described in terms of singly excited configurations. We expect that the quality of these results will depend on the magnitude of spin-contamination and on the effective degree of orbital localization.

In the light of the above considerations, we have selected a number of open-shell singlet diradicals displaying medium to large diradical character and have computed their excited states with standard TDDFT and TDUDFT calculations employing the Gaussian09 suite of programs.[47]

Double excitations can be recovered in TDDFT calculations also with the SF approach.[43,45] Therefore, in addition to the TDUDFT calculations we also carried out SF TDDFT calculations in the collinear approximation as implemented in the Gamess package.[48] In this latter case, the excitation energy to the double exciton state was computed as the energy difference between the singlet ground state and the singlet excited state, both eigenvalues resulting from SF calculations.

Results and Discussion

Ground state structures, diradical and multi-radical character.

All the systems in Fig. 1 display a more stable BS structure (see Table 1) with TPQ, QANTHENE and SHZ showing the larger energy difference between BS and CS structures. The CS and BS equilibrium structures, determined at B3LYP/6-31G* and CAM-B3LYP/6-31G* level, are collected in Figs. S1-S8. It is interesting to explore the correlation between computed geometries and diradical character and between the latter index and the computed BS-CS energy difference.

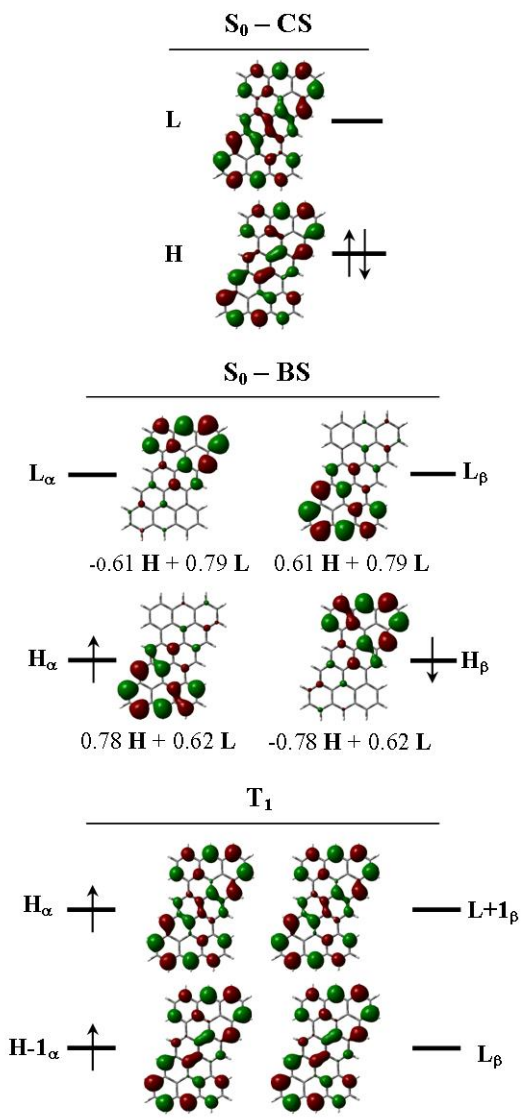

Fig. 4. Frontier molecular orbitals of SHZ computed with (top) a CS singlet reference configuration, (middle) a BS spin-paired open-shell configuration and (bottom) a triplet configuration, at the optimized BS UB3LYP geometry of the singlet ground state ($y_0(PUHF) = 0.87$). Each localized orbital (BS) is also expressed as a linear combination of the delocalized (CS) orbitals.

The diradical character computed at PUHF level (see Table 2) is remarkably dependent on the chosen geometry. The CS CAM-B3LYP geometries correspond (for all the systems investigated) to the smallest diradical character, followed by the CS B3LYP structures. The diradical character increases, as expected, when moving to BS geometries and very similar values are obtained for BS B3LYP or CAM-B3LYP equilibrium structures, with the diradical character of the latter being only slightly larger than that of the former. Thus, although the PUHF diradical character of equilibrium structures determined at CS level, with different functionals, can be quite different (as it happens for instance for 2TIO, FP, TPQ), all functionals lead to BS structures that converge to a similar y_0 value, weakly dependent on the functional (compare for instance the PUHF y_0 values computed for CAM-B3LYP and B3LYP BS structures of FP, DFB, BISPHE, TPQ, SHZ, QANTHENE).

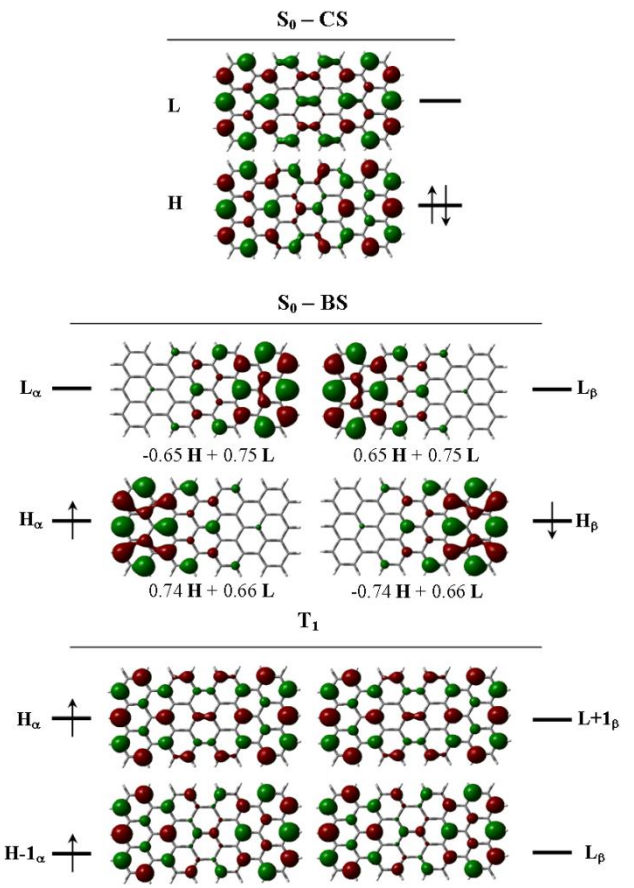

Fig. 5. Frontier molecular orbitals of QANTHENE computed with (top) a CS singlet reference configuration, (middle) a BS spin-paired open-shell configuration and (bottom) a triplet configuration, at the optimized BS UB3LYP geometry of the singlet ground state ($y_0(PUHF) = 0.92$). Each localized orbital (BS) is also expressed as a linear combination of the delocalized (CS) orbitals.

Table 3 Comparison of computed TDB3LYP and TDUUB3LYP excitation energies of the strongly one-photon active excited state (single exciton state or *(H→L)*) and the available experimental data for the systems investigated.

Excited state character →	*(H→L)*	*(H→L)*	*(H→L)*	*(H→L)*
Type of calculation →	*TD-B3LYP/6-31G**	*TD-B3LYP/6-31G**	*TD-UB3LYP/6-31G**	*exp*
Geometry →	*CS B3LYP* [a]	*BS B3LYP* [a]	*BS B3LYP* [a]	
2TIO	1.98	1.86	1.81	1.88[b]
QDTBDT	1.89	1.75	1.81	1.85[c]
FP	1.47	1.32	1.51	1.48[d]
DFB	1.13	1.01	1.13	1.25[e]
BISPHE	1.38	1.35	1.47	1.43[f]
TPQ	1.59	1.44	1.48	1.46[g]
SHZ	1.11	1.01	1.49	1.50[h]
QANTHENE	0.87	0.77	1.28	1.35[i]

[a] Geometry optimized at B3LYP/6-31G* (CS) or UB3LYP/6-31G* (BS) levels of theory; [b]In n-hexane from ref. [38]; [c]Measured in $CHCl_3$ from ref. [27]; [d]In CH_2Cl_2, from ref. [26]; [e]In CH_2Cl_2 from ref. [23]; [f]In $CHCl_3$, from ref [13] [g]Measured in CH_2Cl_2 from ref. [19]; [h]In CH_2Cl_2 from ref. [24]; [i]In CH_2Cl_2 from ref. [21].

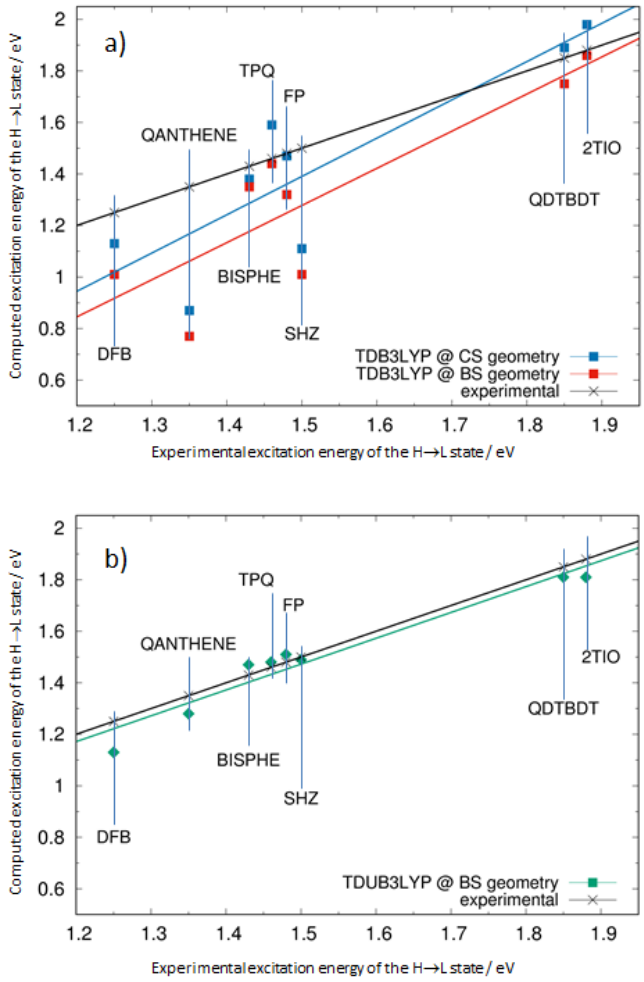

Fig. 6. Computed excitation energy of the one-photon active (H→L) state versus experimental excitation energy: a) TDB3LYP calculations: (blue squares) TDB3LYP at CS geometry; (red squares) TDB3LYP at BS geometry; (black crosses) experimental values; b) (green diamonds) TDUB3LYP at BS geometry; (black crosses) experimental values. The lines in the same colours are linear fittings of the computed data. The black line is the bisector of the graph. Vertical bars indicate the compound to which computed and experimental data correspond.

As expected, the molecules displaying the larger y_0 (QANTHENE, TPQ, SHZ) are also those displaying the larger BS-CS stabilization energy and generally an approximately linear correlation between the diradical character and computed BS stabilization is found (see Fig. 3 and S9).

Fig. 3 shows also that the computed y_0 values, for a given molecule and a selected equilibrium structure, are strongly dependent on the chosen model (PUHF or PUDFT). The y_0 values computed with the PUB3LYP method are always much smaller than those computed at PUCAM-B3LYP level, in turn smaller that the PUHF values (see Table 2). Nevertheless, for the set of molecules investigated, the trend is very similar at all levels of theory considered: 2TIO and QDTBDT show invariably the lowest y_0 values while QANTHENE shows the largest y_0 value at PUHF, PUB3LYP or PUCAM-B3LYP levels. For other molecules in the set, however, the relative position is not the

same at all levels of theory. Notable in this regard is BISPHE whose BS equilibrium structure displays the third lowest y_0 value (PUB3LYP and PUCAM-B3LYP) while it is located among the higher y_0 values at PUHF level. In conclusion the absolute magnitude of y_0 is strongly dependent on geometrical parameters and strongly dependent on the level of theory employed to evaluate the index. It is therefore important to refer precisely to the method and geometry employed to calculate the diradical character. Nevertheless, except for few cases such as BISPHE, the relative y_0 values are consistent for different levels of theory. In the following discussion, we generally take as reference the PUHF value unless specified. For the systems investigated we also evaluated the tetraradical character and the number of unpaired electrons (see Table S2 and S3) both of which are far less dependent on geometry compared to y_0, although still strongly dependent on the level of theory (PUHF, PUDFT) and functional used.

Excited states from TDDFT calculations

As pointed out in a previous section, the molecules in Fig. 1 are simplified models, owning the same conjugated core of the real molecules that were characterized by absorption spectroscopy [13,18,19,21,23,24,26,27]. In the following we will refer to the real molecules with the same label used for the model molecule in Fig. 1. Weak features on the red side of the main strong absorption band were assigned to the double exciton state for 2TIO, TPQ, QANTHENE, SHZ, DFB and FP. Similarly, the electronic absorption spectrum of QDTBDT shows few weak features on the red side (1.57 eV) of the strong absorption at 1.85 eV.[27] Based on the following calculations we propose that these features are due, also in this case, to the double exciton state. In contrast, the electronic absorption spectrum of BISPHE does not show features on the red side of the strong absorption observed at 1.43 eV, but a two photon active state has been observed at 1.54 eV and assigned to the double exciton state.[13]

For the systems in Fig. 1 we have carried out three sets of TDDFT calculations: 1) using a CS reference configuration, at the CS optimized geometry and at the BS optimized geometry; 2) TDUDFT calculations using a BS reference configuration at the BS optimized geometry and, 3) SF TDDFT calculations carried out with a triplet reference configuration at the same BS optimized geometry as above. The B3LYP functional was selected for these calculations owing to its generally good performance for large conjugated systems [49-51] in conjunction with its generally smaller spin contamination compared to hybrid functionals with larger contributions of HF exchange. [52]

Molecular orbitals from RDFT and UDFT calculations. In Figs. 4, 5 and S10-S15, we collect the frontier MOs obtained from 1) CS B3LYP/6-31G* calculations, 2) spin-paired (singlet) open-shell BS UB3LYP/6-31G* calculations and 3) spin-parallel (triplet) UB3LYP/6-31G* calculations, for each system investigated. These sets constitute the MOs used to build the reference configurations in the three sets of TDDFT calculations outlined above. Generally the triplet UDFT MOs are delocalized and similar to the CS MOs. In contrast, BS MOs from unrestricted spin-paired calculations are localized and in each figure we include, for each localized orbital, the linear combinations of CS delocalized orbitals to which it corresponds. The degree of localization between pairs of HOMOα/HOMOβ LUMOα/LUMOβ orbitals and the degree of similarity between HOMOα and LUMOβ (or HOMOβ and LUMOα) is established by evaluating their overlap (Table S4).

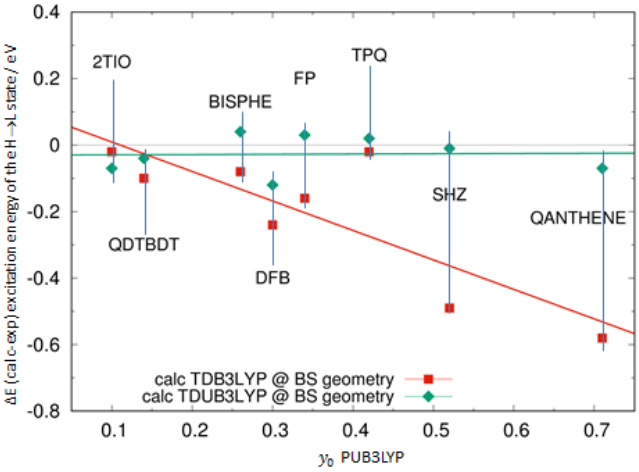

Fig. 7. Difference between computed and observed excitation energy of the one-photon active (H→L) state versus computed diradical character at PUB3LYP level: (red squares) TDB3LYP at BS B3LYP geometry; (green diamonds) TDUB3LYP at the same geometry. The lines in the same colours are linear fittings of the computed data. Vertical bars indicate the compound to which computed data correspond.

Table 4 Computed TDUDFT and SF TDDFT excitation energies of the one-photon forbidden excited state (double exciton state or *(H,H→L,L))* for the systems investigated.

Excited state character →	*(HH→LL)*	*(HH→LL)*	*(HH→LL)*
Type of calculation →	*TDUB3LYP/ 6-31G**	*SF TDB3LYP/ 6-31G**	*exp*
Geometry →	*BS CAM-B3LYP* [a]	*BS CAM-B3LYP* [a]	
2TIO	0.98	1.54	1.68[b]
QDTBDT	1.07	1.56	1.57[c]
FP	1.13	1.05	1.13[d]
DFB	0.91	0.86	0.92[e]
BISPHE	1.03	1.27	1.54[f]
TPQ	1.16	1.04	1.13[g]
SHZ	1.32	0.98	1.19[h]
QANTHENE	1.17	0.76	1.08[i]

[a]Geometry optimized at UB3LYP/6-31G* (BS) levels of theory [b]In n-hexane from ref. [38]; [c]Measured in $CHCl_3$ from ref. [27]; [d]In CH_2Cl_2, from ref. [26]; [e]In CH_2Cl_2 from ref. [23]; [f]In $CHCl_3$, from ref [13] [g]Measured in CH_2Cl_2 from ref. [19]; [h]In CH_2Cl_2 from ref. [24]; [i]In CH_2Cl_2 from ref. [21].

We note that 2TIO and QDTBDT are the systems with the smaller diradical character in the series. The smaller y_0 is reflected in a modest localization of the BS MOs (see Figs. S10-S15) compared to those of the systems displaying the larger diradical character, as SHZ and QANTHENE, (see Figs. 4 and 5)

which are strongly localized, thereby implying that, in these cases, we are close to the ideal conditions of the 2e-2o model.

Predictions for the single exciton state. From TDB3LYP calculations we expect a good quality prediction of the lowest strongly dipole allowed excited state dominated by the (H→L) excitation. Indeed, the data collected in Table 3 (for B3LYP geometries) and Table S5 (for CAM-B3LYP geometries) show generally a good agreement with the experimental results.

The excitation energies in Table 3, computed from TDB3LYP calculations for two sets of geometries (CS and BS determined with the B3LYP functional), are plotted against the experimental data in Fig. 6a. To easily capture a trend in the computed results, we fitted them linearly, keeping in mind that the computed data may be affected by systematic errors due to the simplifications of the models compared to the real systems and the absence of solvent effects. It can be seen that the linear fittings of the two sets of computed excitation energies (blue and red squares) are almost parallel, which indicates a similar average quality of the results, with an energy shift due to the systematic difference in geometry between the two sets. The only two data showing a stronger deviation from the fitting correspond to QANTHENE and SHZ, the two compounds with the largest diradical character and consequently those more affected by static correlation which is missing for a CS single reference as that used in these TDB3LYP calculations.

In contrast, the green diamonds and the green fitting line in Fig. 6b (TDUB3LYP predictions, see also Table 3 and S6 for additional details) show a different slope, almost parallel with the bisector of the graph (thin black line), thereby indicating minor average deviations from the experimental data (also shown as black crosses on the bisector). The good agreement with the experiment, independent of the diradical character, can be appreciated in Fig. 7 where the difference between computed and observed excitation energies are reported as a function of the PUB3LYP y_0 value (in this case we used the PUB3LYP values since these are computed at same level of theory employed for the TDDFT calculations). The better quality of TDUB3LYP calculations is evident for systems with large diradical character such as SHZ and QANTHENE, for which TDB3LYP calculations provide strongly underestimates. We attribute the better agreement of TDUB3LYP calculations to the use of an unrestricted reference configuration which is able to recover static correlation effects in spite of some degree of spin contamination (see Table S6).

Predictions for the double exciton state. The double exciton state has been previously identified and described in terms of high level quantum chemical calculations. CASPT2//CASSCF calculations were carried out for 2TIO [38] and TPQ [40] while CASSCF followed by NEVPT2 calculations were carried out for QANTHENE. [21] All the previous high level calculations predicted excitation energies of the double exciton state very close to the experimentally observed values, thereby supporting the proposed assignment. As a result we may confidently compare the results of the TDDFT calculations presented here with the experimental data. More precisely, in Table 4 (for B3LYP geometries) and Table S5 (for CAM-B3LYP geometries) we collect the computed excitation energies of the double exciton state (H,H→L,L) obtained from TDUB3LYP calculations and SF TDB3LYP calculations (both carried out at the BS equilibrium structures) and compare them with available experimental data. The computed SF TDB3LYP excitation energies are plotted against experimental values in Fig. 8 (red squares). Also in this case we fitted them linearly to easily capture a trend: the red line is almost parallel to that of the experimental values (black line), indicating an average similar accuracy for the set of diradicals considered, but a general underestimate of excitation energies which may be related to the overestimate of the ground state energy at this level of theory.

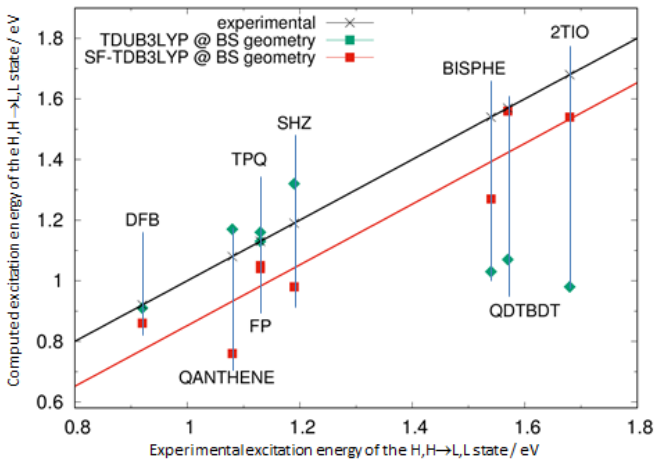

Fig. 8. Computed excitation energy of the one-photon forbidden (H,H→L,L) excited state versus experimental excitation energy: (red squares) SF TDB3LYP at BS geometry; (green diamonds) TDUB3LYP at BS geometry; (black crosses) experimental values. The lines in the same colours are linear fittings of the computed data. The TDUB3LYP data were not fitted due to their different quality for the two groups of systems investigated (see the text for the discussion). The black line is the bisector of the graph. Vertical bars indicate the compound to which computed and experimental data correspond.

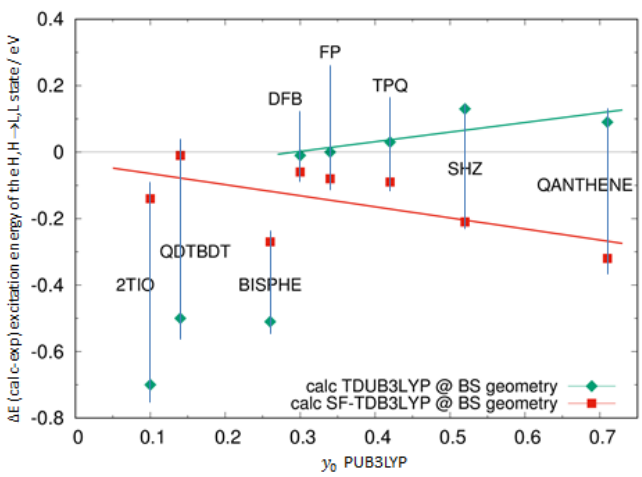

Fig. 9. Difference between computed and observed excitation energy of the one-photon forbidden (H,H→L,L) state versus the computed diradical character at PUB3LYP level: (red squares) SF TDB3LYP at BS B3LYP geometry; (green diamonds) TDUB3LYP at the same geometry. The lines in the same colours are linear fittings of the computed data. Vertical bars indicate the compound to which computed data correspond.

The difference between computed and observed excitation energy, plotted against the PUB3LYP diradical character in Fig. 9 discloses, in addition to the underestimate, a slight accuracy decrease of SF TDB3LYP results as the diradical character increases, likely due to the imperfect description of static correlation for large y_0. The green diamonds in Fig. 8 correspond to TDUB3LYP computed excitation energies of the double exciton state, identified by the dominant in phase contribution of the singly excited configurations A^2 and B^2, (see Table S7 for additional details on computed spin contamination, wavefunction composition and oscillator strengths) as discussed in the previous section and shown in Fig. 2. For five, out of the eight systems investigated, the TDUB3LYP results are in very close agreement with experimental data, almost overlapping with the bisector line in Fig. 8, while for 2TIO, QDTBDT and BISPHE the computed excitation energies are strongly underestimated. 2TIO and QDTBDT are the systems with the smaller diradical character in the series, either at PUHF or PUB3LYP level (see Table 2), in turn reflected in a modest localization of the BS UB3LYP frontier MOs which implies an imperfect representation of the 2e-2o model in the localized basis set (the overlap between HOMOα and HOMOβ amounts to 0.57 and 0.52 respectively, see Table S4). BISPHE also displays less localized UB3LYP frontier MOs (the overlap between HOMOα and HOMOβ amounts to 0.41, see Fig. S14 and Table S4) in agreement with the fact that the PUB3LYP y_0 value is just above that of 2TIO and QDTBDT, as noted in a previous section. Inspection of Table S7 shows that the S^2 value of the double exciton state in these three cases does not exceed 0.7. Although triplet spin contamination may contribute to the energy underestimate, it is likely that the identical contribution of ground and doubly excited configurations leads to the large underestimate of the excitation energy since the contribution of the doubly excited configuration should dominate when orbitals tend to be delocalized.[8] In contrast, the more marked localization of the frontier MOs of SHZ and QANTHENE (the HOMOα/HOMOβ overlap is only 0.23 and 0.11, respectively) implies that in this case we are close to the ideal conditions of the 2e-2o model. The BS reference configuration recovers, via localization, the static correlation which is missing in the CS reference configuration and, on the other hand, the appropriate combination of singly excited configurations between localized orbitals, A^2 and B^2, (see Table S7) corresponds to the double exciton state in eq.(4). The S^2 value of the double exciton state in these favourable cases (Table S7) remains always around 0.3-0.4 which implies a moderate triplet spin contamination. We believe that the combination of strong localization of frontier MOs and inclusion of static correlation effects justifies the remarkably good predictions of TDUB3LYP compared to SF TDB3LYP for diradicals with very large y_0 values (see also Fig. 9 showing that TDUB3LYP is superior to SF TDB3LYP for large diradical character). On the other hand we note that when the localization is incomplete, as is the case of 2TIO and QDTBDT, the description of the double exciton state rapidly deteriorates due to an increased role of triplet spin contamination and/or unbalanced contribution of the ground and doubly excited configurations in the wavefunction. Although inspection of data in Fig. 9 suggests that for y_0 values (PUB3LYP level) above 0.3 the predicted excitation energies are very satisfactory, we believe that the most relevant parameter to be monitored for a safe prediction is orbital localization. We can therefore conclude that the TDUDFT approach should not be used to estimate the excitation energy of the double exciton state when the diradical character is small and/or orbital localization is incomplete.

Conclusions

A specific characteristic of open-shell singlet diradical molecules is the presence of a double exciton state H,H→L,L among low lying excited states. While the simple 2e – 2o model predicts the double exciton state to lie above the single exciton H→L state, recent high-level quantum-chemical investigations including static and dynamic electron correlation have demonstrated that the double exciton state can become the lowest singlet excited state for systems with large diradical character. In this work we have investigated the less computationally demanding TDDFT calculations as an alternative to characterize the low lying singlet excited states of recently synthesized large polyconjugated diradicals. TDDFT based on the restricted CS or unrestricted BS antiparallel-spin reference configurations have been compared for the prediction of the excitation energy of the bright H→L state. To obtain the excitation energy of the double exciton state we have employed the same TDUDFT calculations used for the single exciton prediction along with the SF TDDFT approach. We selected the B3LYP functional because of its limited spin contamination compared to other functionals. While it is known that SF TDDFT calculations can predict electronic states whose wavefunction includes double excitations, we have shown that the double exciton state characterizing open shell singlet diradicals can be captured by TDUB3LYP calculations, when the diradical character is large, since it corresponds to single excitations from strongly localized frontier MOs.

A systematic investigation encompassing a set of recently synthesized large conjugated systems displaying from moderate to large diradical character and an open-shell singlet ground state, shows that TDUB3LYP predicted excitation energies of the bright, single exciton state are in average better agreement with experiment compared to TDB3LYP results.

Focussing on the dark double exciton state, calculations show that the SF approach in the collinear approximation provides an overall good prediction of its excitation energy across the set of diradicals investigated, although computed data are underestimated with respect to the experimental results. The predicted excitation energies are in excellent agreement with experiment when TDUB3LYP calculations are carried out for systems whose diradical character is large and whose BS frontier MOs are strongly localized. In these cases not only the calculations predict, in agreement with experimental observation and with higher level calculations, that the double exciton state lies below the single exciton state, but locate its

energy with great accuracy. In contrast, the quality decreases for moderate diradical character and incomplete localization of frontier MOs. Therefore TDUB3LYP calculations can be used to predict the double exciton state provided the diradical character is large enough to ensure strong orbital localization. In conclusion, both SF TDB3LYP and TDUB3LYP calculations can be considered suitable and computationally cheaper alternatives to characterize the low lying double exciton state of singlet open shell conjugated diradicals of large dimension. SF TDB3LYP performs better for small to medium diradical character than for large diradical character, likely because of the imperfect description of static correlation for large y_0. In contrast, a large diradical character, (and strong orbital localization) is a prerequisite for the success of TDUB3LYP calculations whose quality otherwise deteriorates.

Conflicts of interest

There are no conflicts to declare.

Acknowledgements

Financial support from MINECO, Spain project reference CTQ2015-69391-P and RFO funds from the University of Bologna are acknowledged. We thank G. Visentin for preliminary calculations carried out on 2TIO and QANTHENE.

Notes and references

1 Z. Sun, Z. Zeng and J. Wu, "Zethrenes, extended *p*-Quinodimethanes, and Periacenes with a Singlet Biradical Ground State" *Acc. Chem. Res*. 2014, **47**, 2582–2591.
2 Z. Zeng, X. Shi, C. Chi, J. T. Lopez Navarrete, J. Casado and J. Wu, "Pro-Aromatic and Anti-Aromatic π-Conjugated Molecules: An Irresistible Wish to Be Diradicals", *Chem. Soc. Rev*., 2015, **44**, 6578.
3 T. Kubo, "Recent Progress in Quinoidal Singlet Biradical Molecules", *Chem. Lett*., 2015, **44**, 111–122.
4 M. Nakano and B. Champagne, "Theoretical Design of Open-Shell Singlet Molecular Systems for Nonlinear Optics", *J. Phys. Chem. Lett.* 2015, **6**, 3236–3256.
5 G. E. Rudebusch, J. L. Zafra, K. Jorner, K. Fukuda, J. L. Marshall, I. Arrechea-Marcos, G. L. Espejo, R. P. Ortiz, C. J. Gómez-García, L. N. Zakharov, M. Nakano, H. Ottosson, J. Casado, M. M. Haley, "Diindeno-fusion of an anthracene as a design strategy for stable organic biradicals" *Nature Chem.* 2016, **8**, 753–759.
6 R. P. Ortiz, A. Facchetti, T. J. Marks, J. Casado, M. Z. Zgierski, M. Kozaki, V. Hernandez and J. T. L. Navarrete, "Ambipolar Organic Field-Effect Transistors from Cross-Conjugated Aromatic Quaterthiophenes; Comparisons with Quinoidal Parent Materials" *Adv. Funct. Mater.* 2009, **19**, 386-394.
7 M. Nakano, "Open-Shell-Character-Based Molecular Design Principles: Applications to Nonlinear Optics and Singlet Fission" *Chem. Rec*. 2017, **17**, 27-62
8 M. Nakano, "*Excitation Energies and Properties of Open-Shell Singlet Molecules*", SpringerBriefs in Molecular Science, Springer, 2014.
9 T. Minami and M. Nakano, "Diradical Character View of Singlet Fission", *J. Phys. Chem. Lett*., 2012, **3**, 145-150.
10 S. Ito, T. Nagami and M. Nakano, "Molecular design for efficient singlet fission", *J. Photochem. Photobiol. C: Photochem. Rev*., 2018, **34**, 85-120.
11 K. Yamaguchi, in *Self-Consistent Field: Theory and Applications*, ed. R. Carbo and M. Klobukowski, Elsevier, Amsterdam, The Netherands, 1990, p. 727.
12 K. Yamaguchi, "The Electronic Structures of Biradicals in the Unrestricted Hartree-Fock Approximation", *Chem. Phys. Lett*. 1975, **33**, 330-335.
13 K. Kamada, K. Ohta, A. Shimizu, T. Kubo, R. Kishi, H. Takahashi, E. Botek, B. Champagne and M. Nakano, "Singlet Diradical Character from Experiment", *J. Phys. Chem. Lett.* 2010, **1**, 937-940.
14 Z. Sun and J. Wu, "Open-shell polycyclic aromatic hydrocarbons", *J. Mater. Chem.*, 2012, **22**, 4151–4160.
15 T. Y. Gopalakrishna, W. Zeng, X. Lu and J. Wu, "From open-shell singlet diradicaloids to polyradicaloids", *Chem. Commun.*, 2018, **54**, 2186-2199.
16 T. Takahashi, K. Matsuoka, K. Takimiya, T. Otsubo and Y. Aso, "Extensive Quinoidal Oligothiophenes with Dicyanomethylene Groups at Terminal Positions as Highly Amphoteric Redox Molecules", *J. Am. Chem. Soc.*, 2005, **127**, 8928-8929.
17 R. P. Ortiz, J. Casado,; S. R. Gonzalez, V. Hernandez, J. T. L. Navarrete, P. M. Viruela, E. Orti, K. Takimiya and T. Otsubo, "Quinoidal Oligotiophenes: towards biradical ground-state species", *Chem. Eur. J.* 2010, **16**, 470-484.
18 D. Fazzi, E. V. Canesi, F. Negri, C. Bertarelli and C. Castiglioni, "Biradicaloid Character of Thiophene-Based Heterophenoquinones: The Role of Electron-Phonon Coupling", *ChemPhysChem*, 2010, **11**, 3685-3695.
19 X. Zhu, H. Tsuji, K. Nakabayashi, S.-i Ohkoshi and E. Nakamura, "Air- and Heat-Stable Planar Tri-*p*-quinodimethane with Distinct Biradical Characteristics", *J. Am. Chem. Soc.* 2011, **133**, 16342-16345.
20 T. Kubo, A. Shimizu, M. Uruichi, K. Yakushi, M. Nakano, D. Shiomi, K. Sato, T. Takui, Y. Morita and K. Nakasuji, "Singlet Biradical Character of Phenalenyl-Based Kekule´ Hydrocarbon with Naphthoquinoid Structure", *Org. Lett*., 2007, **9**, 81-84.
21 A. Konishi, Y. Hirao, K. Matsumoto, H. Kurata, R. Kishi, Y. Shigeta, M. Nakano, K. Tokunaga, K. Kamada and T. Kubo, "Synthesis and Characterization of Quarteranthene: Elucidating the Characteristics of the Edge State of Graphene Nanoribbons at the Molecular Level", *J. Am. Chem. Soc*. 2013, **135**, 1430-1437.
22 J. Liu, P. Ravat, M. Wagner, M. Baumgarten, X. Feng and K. Müllen, "Tetrabenzo[a,f,j,o]perylene: A Polycyclic Aromatic Hydrocarbon With An Open-Shell Singlet Biradical Ground State", *Angew. Chem. Int. Ed*., 2015, **54**, 12442-12446.
23 J. Ma, J. Liu, M. Baumgarten, Y. Fu, Y-Z. Tan, K. S. Schellhammer, F. Ortmann, G. Cuniberti, H. Komber, R. Berger, K. Müllen and X. Feng, "A Stable Saddle-Shaped Polycyclic Hydrocarbon with an Open-Shell Singlet Ground State", *Angew. Chem. Int. Ed*., 2017, **129**, 3328-3332.
24 W. Zeng, Z. Sun, T. S. Herng, T. P. Gonçalves, T. Y. Gopalakrishna, K.-W. Huang, J. Ding and J. Wu, "Super-heptazethrene", *Angew. Chem. Int. Ed*., 2016, **55**, 8615-8619
25 P. Ravat, T. Šolomek, M. Rickhaus, D. Häussinger, M. Neuburger, M. Baumgarten and M. Juríček, "Cethrene: A Helically Chiral Biradicaloid Isomer of Heptazethrene", *Angew. Chem. Int. Ed*., 2016, **55**, 1183-1186.
26 P. Hu, S. Lee, T. S. Herng, N. Aratani, T. P. Gonçalves, Q. Qi, X. Shi, H. Yamada, K.-W. Huang, J. Ding, D. Kim and J. Wu, "Toward Tetraradicaloid: The Effect of Fusion Mode on Radical Character and Chemical Reactivity", *J. Am. Chem. Soc.*, 2016, **138**, 1065–1077.

27 J. Li, X. Qiao, Y. Xiong, H. Li and D. Zhu, "Five-Ring Fused Tetracyanothienoquinoids as High-Performance and Solution-Processable n−Channel Organic Semiconductors: Effect of the Branching Position of Alkyl Chains", *Chem. Mater.*, 2014, **26**, 5782-5788
28 D. Xia, A. Keerthi, C. An and M. Baumgarten, "Synthesis of a quinoidal dithieno[2,3-d;2',3'-d]benzo[2,1-b;3,4-b']-dithiophene based open-shell singlet biradicaloid", *Org. Chem. Front*., 2017, **4**, 18-21.
29 F. Bell, P. M. Zimmerman, D. Casanova, M. Goldey and M. Head-Gordon, "Restricted active space spin-flip (RAS-SF) with arbitrary number of spin flips", *Phys. Chem. Chem. Phys*., 2013, **15**, 358-366.
30 S. Das, T. S. Herng, J. L. Zafra, P. Mayorga Burrezo, M. Kitano, M. Ishida, T. Y. Gopalakrishna, P. Hu, A. Osuka, J. Casado, J. Ding, D. Casanova and J. Wu, "Fully Fused Quinoidal/Aromatic Carbazole Macrocycles with Poly-radical Characters", *J. Am. Chem. Soc*., 2016, **138**, 7782-7790.
31 A. Perez-Guardiola, M. E. Sandoval-Salinas, D. Casanova, E. San-Fabian, A. J. Perez-Jimenez and J. C. Sancho-Garcia, "The role of topology in organic molecules: origin and comparison of the linear character in linear and cyclic oligoacenes and related oligomers" *Phys. Chem. Chem. Phys*., 2018, **20**, 7112-7124.
32 F. Plasser, H. Pasalic, M. H. Gerzabek, F. Libisch, R. Reiter, J. Burgdörfer, T. Müller, R. Shepard, H. Lischka, "The Multiradical Character of One- and Two-Dimensional Graphene Nanoribbons" *Angew. Chem., Int. Ed.* 2013, **52**, 2581−2584.
33 A. Das, T. Müller, F. Plasser, H. Lischka, "Polyradical Character of Triangular Non-Kekulé Structures, Zethrenes, p-Quinodimethane-Linked Bisphenalenyl, and the Clar Goblet in Comparison: An Extended Multireference Study" *J. Phys. Chem. A,* 2016, **120**, 1625−1636.
34 P. M. Lahti, A. S. Ichimura and J. A. Sanborn, "Methodologies for Computational Studies of Quinoidal Diiminediyls: Biradical vs Dinitrene Behavior", *J. Phys. Chem. A*, 2001, **105**, 251-260.
35 L. Salem, C. Rowland, "The electronic properties of diradicals", *Angew. Chem. Int. Ed.*, 1972, **11**, 92.
36 V. Bonačić-Koutecký, J. Koutecký and J. Michl, "Neutral and Charged Biradicals, Zwitterions, Funnels in S_1, and Proton Translocation: Their Role in Photochemistry, Photophysics, and Vision" *Angew. Chem. Int. Ed. Engl*., 1987, **26**, 170-189.
37 L. V. Slipchenko and A. I. Krylov, "Singlet-triplet gaps in diradicals by the spin-flip approach: A benchmark study", *J. Chem. Phys*., 2002, **117**, 4694-4708.
38 S. Di Motta, F. Negri, D. Fazzi, C. Castiglioni and E. V. Canesi, "Biradicaloid and Polyenic Character of Quinoidal Oligothiophenes Revealed by the Presence of a Low-Lying Double-Exciton State", *J. Phys. Chem. Lett*. 2010, **1**, 3334-3339.
39 K. Schulten and M. Karplus, "On The Origin of a Low-Lying Forbidden Transition in Polyenes and Related Molecules", *Chem. Phys. Lett*., 1972, **14**, 305-309.
40 R. C. González-Cano, S. Di Motta, X. Zhu, J. T. López Navarrete, H. Tsuji, E. Nakamura, F. Negri and J. Casado, "Carbon-Bridged Phenylene-Vinylenes: On the Common Diradicaloid Origin of Their Photonic and Chemical Properties", *J. Phys. Chem. C*, 2017, **121**, 23141-23148.
41 A. Charaf-Eddin, A. Planchat, B. Mennucci, C. Adamo and D. Jacquemin, "Choosing a Functional for Computing Absorption and Fluorescence Band Shapes with TD-DFT", *J. Chem. Theory Comput*., 2013, **9**, 2749-2760.
42 D. Jacquemin, B. Moore, A. Planchat, C. Adamo and J. Autschbach, "Performance of an Optimally Tuned Range-Separated Hybrid Functional for 0−0 Electronic Excitation Energies", *J. Chem. Theory Comput*., 2014, **10**, 1677−1685.
43 Y. Shao, M. Head-Gordon and A. I. Krylov, " The spin-flip approach within time-dependent density functional theory: Theory and applications to diradicals", *J. Chem. Phys.*, 2003, **118**, 4807-4818.
44 K. D. Nanda and A. I. Krylov, "Effect of the diradical character on static polarizabilities and two-photon absorption cross sections: A closer look with spin-flip equation-of-motion coupled-cluster singles and doubles method", *J. Chem. Phys*., 2017, **146**, 224103.
45 Z. Rinkevicius, O. Vahtras and H. Ågren, "Spin-flip time dependent density functional theory applied to excited states with single, double, or mixed electron excitation character", *J. Chem. Phys*., 2010, **133**, 114104.
46 M. Head-Gordon, "Characterizing unpaired electrons from the one-particle density matrix", *Chem. Phys. Lett*., 2003, **372**, 508-511.
47 M. J. Frisch, et al., Gaussian 09 Revision D.01, Gaussian Inc., Wallingford CT, 2009.
48 M. W. Schmidt, K. K. Baldridge, J. A. Boatz, S. T. Elbert, M. S. Gordon, J. H. Jensen, S. Koseki, N. Matsunaga, K. A. Nguyen, S. J. Su, T. L. Windus, M. Dupuis and J. A. Montgomery, "General atomic and molecular electronic structure system", *J. Comput. Chem*., 1993, **14**, 1347-1363.
49 H. Qian, F. Negri, C. Wang and Z. Wang, "Fully Conjugated Tri(perylene bisimides): An Approach to the Construction of *n*-Type Graphene Nanoribbons", *J. Am. Chem. Soc*., 2008, **130**, 17970-17976.
50 Y. Li, J. Gao, S. Di Motta, F. Negri, Z. Wang, "Tri-N-annulated Hexarylene: An Approach to Well-Defined Graphene Nanoribbons with Large Dipoles", *J. Am. Chem. Soc*., 2010, **132**, 4208-4213.
51 W. Yue, A. Lv, J. Gao, W. Jiang, L. Hao, C. Li, Y. Li, L. E. Polander, S. Barlow, W. Hu, S. Di Motta, F. Negri, S. R. Marder and Z. Wang, "Hybrid Rylene Arrays via Combination of Stille Coupling and C−H Transformation as High-Performance Electron Transport Materials", *J. Am. Chem. Soc.*, 2012, **134**, 5770−5773.
52 A. S. Menon and L. Radom, "Consequences of Spin Contamination in Unrestricted Calculations on Open-Shell Species: Effect of Hartree-Fock and Møller-Plesset Contributions in Hybrid and Double-Hybrid Density Functional Theory Approaches", J. Phys. Chem. A 2008, 112, 13225–13230